# Modelling the 13.44 GHz Masers in W3(OH)

By MALCOLM GRAY[1]†

[1]Department of Physics & Astronomy, University of Wales, Cardiff, P.O. Box 913, Cardiff, CF2 3YB, UK

I show that Accelerated Lambda Iteration (ALI) radiation transfer models can reproduce gain coefficients, in the 13.44 GHz rotationally excited OH maser, which are consistent with observations. The 13.44 GHz masers have so far been observed uniquely towards the massive star-forming region W3(OH). The pumping of the 13.44 GHz transition is predominantly radiative, via far-infrared lines and a dust continuum. Photochemical pumping may be present, but is not required. The main reason for the failure of LVG models to produce adequate gain-coeffcients at 13.44 GHz is the limitation on optical depth inherent in the LVG approximation.

## 1. Introduction

Maser emission at 13.44 GHz from the $F1, J = 7/2$, rotationally excited state of OH has been observed uniquely from the massive star-forming region W3(OH). Recent VLBI imaging Baudry & Diamond (1998) has shown that the 13.44 GHz emission breaks down into several spatial spots, one of which is very compact, having a linear extent of $<$ 1 AU. Pumping models employing the large velocity gradient (LVG) radiation transfer approximation (for example, Pavlakis & Kylafis 1996; Gray, Field & Doel 1992; Cesaroni & Walmsley 1991) are not able to produce sufficiently large gain coefficients to explain the very compact 13.44 GHz maser spot. This has led some authors to abandon the far infrared (FIR) plus collisional pump in favour of a photochemical model Thissen, Spiecker & Andresen (1999) in which OH with the necessary inverted populations is generated by photodissociation of water released from evaporating ice mantles of dust grains. These 'grains' might have to extend up to cometary dimensions to explain the emission at 13.44 GHz. In this work, I show the effect of replacing the approximate LVG pumping model with a more modern ALI method. Much larger gain coefficients become available, and the FIR pumping model is quite adequate to explain the observed compact 13.44 GHz emission from W3(OH).

## 2. The ALI model

The basic ALI model is derived from code developed by Scharmer & Carlsson (1986), with modifications for analysis of OH from Jones et al. (1994). A dust continuum is included, using dust parameters from Laor & Draine (1993). The model has slab geometry, which in the context of a massive star-forming region, is taken to represent the region between the ionization front bordering the UCHII region of the star, and the shock dividing outflowing material from the cold undisturbed molecular cloud gas. The photodissociation region, dominated by ultraviolet radiation longward of the Lyman limit, forms a subset of the region modelled.

As a first approximation, the model slabs were taken to have uniform physical conditions, except for the velocity shift across the slab, which was varied in some runs. The thickness of the slab was taken to be $2.0\times10^{13}$ m, with the gas at a kinetic temperature of 25 K. Dust temperatures were varied between 50 K and 200 K. The collision partner for the OH was assumed to be molecular hydrogen at number densities from $5\times10^{13}\,\mathrm{m}^{-3}$,

† Present address: Department of Physics, UMIST, P.O. Box 88, Manchester M60 1QD

up to $8\times10^{14}\,\mathrm{m}^{-3}$, with the OH number density adjusted so that every run spanned the indentical range in OH concentration of 0.12 to 2.4 parts per million with respect to $H_2$. A standard velocity shift across the model was $10\,\mathrm{km\,s}^{-1}$, This shift was varied between 10 and $-10\,\mathrm{km\,s}^{-1}$.

## 3. Results of computations

In Figure 1, I show $\Gamma$, the natural logarithm of the unsaturated integrated gain coefficient, as a function of dust temperature and OH concentration. The $H_2$ number density is $2\times10^{14}\,\mathrm{m}^{-3}$ in both Figures. The logarithm of the integrated gain is defined as

$$\Gamma = \Sigma_{i=1}^{N} \gamma_i dz_i \tag{3.1}$$

where $\gamma_i$ is the maser gain coefficient, $dz_i$ the thickness of the $i$-th slab, and there are $N$ slabs in all. Integrated gains are plotted for four maser transitions: the 13.44 GHz line itself, the 13.43 GHz transition which is not observed as a maser, the 6035 MHz line, which is associated with 13.44 GHz, and the ground-state 1665 MHz maser. In Figure 2, I show the variation of the integrated gain as a function of OH concentration and velocity shift across the model slab.

## 4. Conclusions

Increasing dust temperature and increasing OH concentration both act to increase the gain in the excited state lines. Gains are so high that only a small percentage of the modelled cloud need be inverted to produce an intense maser. The behaviour at 1665 MHz is noticeably different. The association of 13.44 GHz and 6035 MHz emission is well reproduced in Figure 1, but a problem for this model is that large gains are also generated at 13.43 GHz, contrary to observations. In Figure 2, it is clear that the largest gains are produced when the velocity shift across the model are small. Any LVG model corresponds, roughly to a high velocity position on these diagrams, so ALI models can access parameter space with larger gains than can LVG.

The author acknowledges with thanks support from the Royal Society, in the form of a 1983 University Research Fellowship.

## REFERENCES

Baudry, A. & Diamond, P. J. 1998 VLBA polarization observations of the $J = 7/2$, 13.44 GHz OH maser in W3(OH) *A&A* **331**, 697–708.

Cesaroni, R. & Walmsley, C.M. 1991 OH maser models revisited *A&A* **241**, 537–550.

Gray, M. D., Field, D. & Doel R. C. 1992 An analysis of intense OH maser emission in star-forming regions *A&A* **262**, 555–569.

Jones, K. N., Field, D., Gray, M. D. & Walker, R.N.F. 1994 OH absorption in FR21 and K3-50 revisited *A&A* **288**, 581–590.

Laor, A. & Draine, B. T. 1993 Spectroscopic constraints on the properties of dust in active galactic nuclei *ApJ* **402**, 441–468.

Pavlakis, K. G. & Kylafis N.D. 1996 OH masers as diagnostics of physical conditions in star-forming regions. II. effects of large velocity gradients and infrared radiation *ApJ* **467**, 309–320.

Scharmer, G. B. & Carlsson, M. 1985 ALI methods *J. Comp. Phys.* **59**, 56–72.

Thissen, T., Spiecker, H. & Andresen, P. 1999 Dynamics of OH masers in regions of star formation I *A&AS* **137**, 323–336.

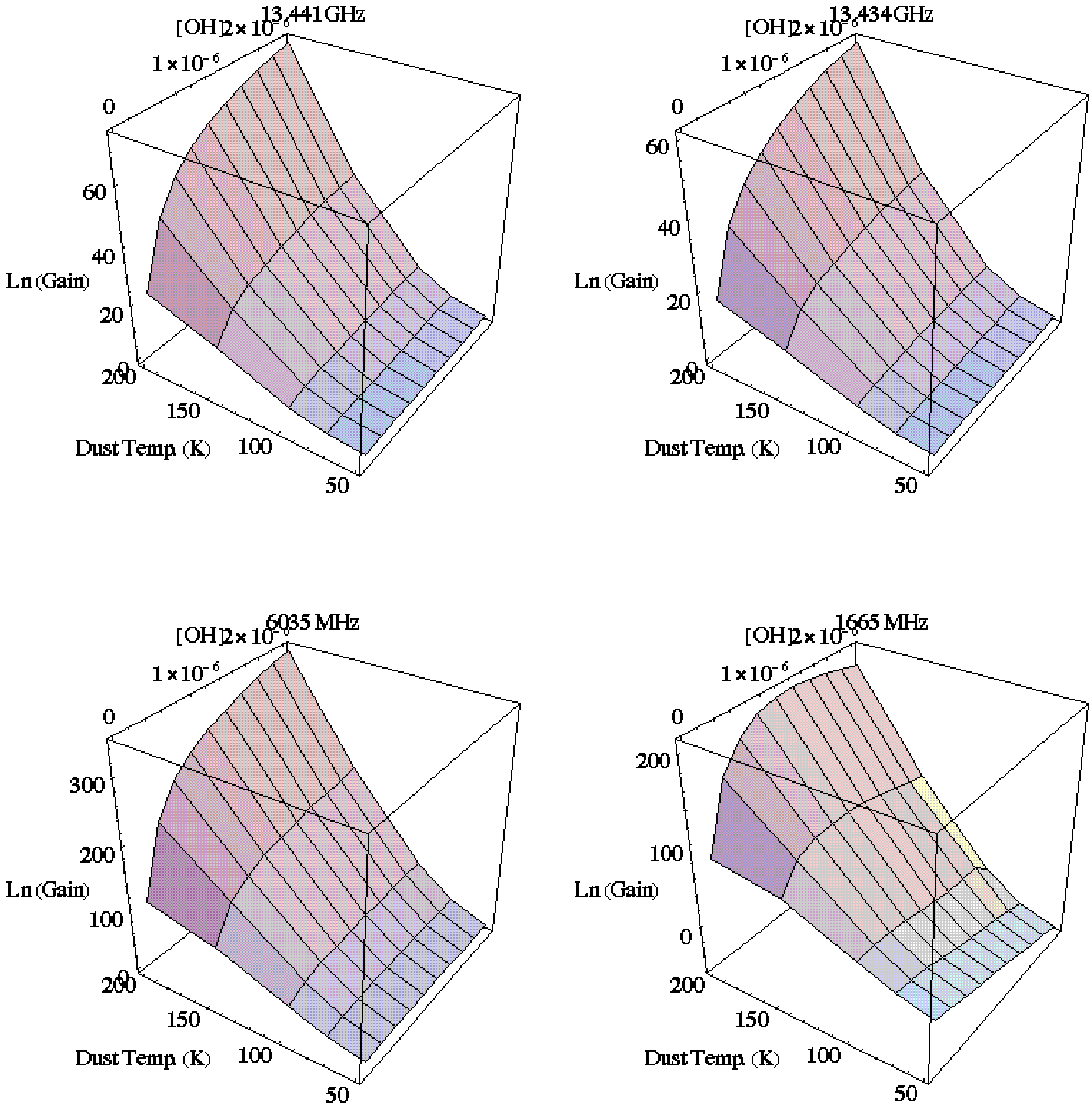


FIGURE 1. The variation of integrated maser gains in various transitions as a function of model parameters. All plots show variation with OH abundance and dust temperature for the 13.44 GHz line observed as a strong maser towards W3(OH); the 13.43 GHz line, observed weakly in absorption towards W3(OH); the 6035 GHz transition; the ground state 1665 MHz transition. In all plots there is a 10 km/s velocity shift, and 80 slabs ($N = 80$).

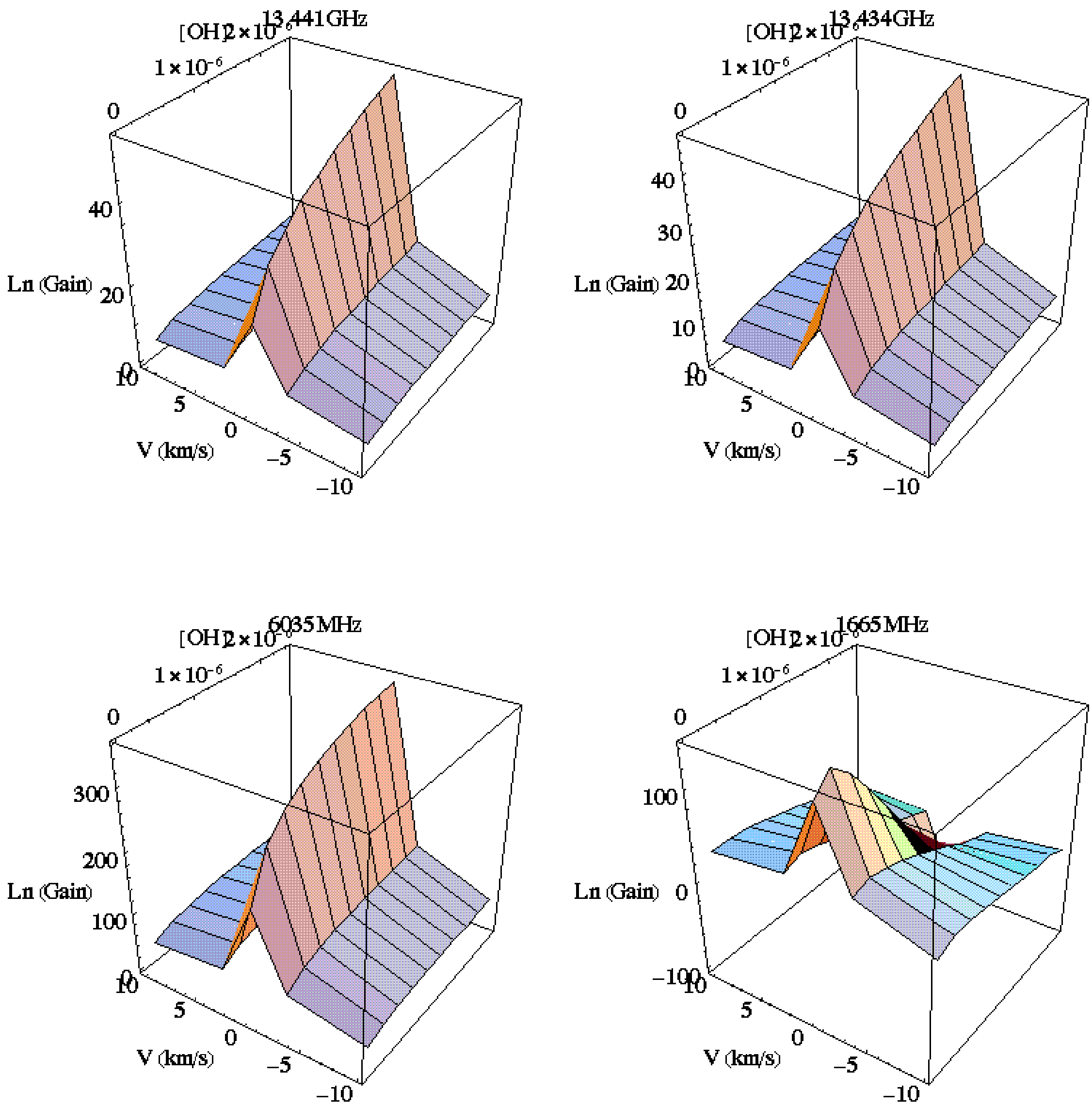


FIGURE 2. The variation of integrated maser gains in various transitions as a function of model parameters. All plots show variation with OH abundance and velocity shift for the 13.44 GHz line observed as a strong maser towards W3(OH); the 13.43 GHz line, observed weakly in absorption towards W3(OH); the 6035 GHz transition; the ground state 1665 MHz transition. In all plots the dust temperature is 100 K.